Author Manuscript

Author Manuscript

Author Manuscript

Author Manuscript

HHS Public Access

Author manuscript

Lab Invest. Author manuscript; available in PMC 2023 May 30.

Published in final edited form as:

Lab Invest. 2022 February ; 102(2): 185–193. doi:10.1038/s41374-021-00700-8.

Evaluation of an EZH2 inhibitor in patient-derived orthotopic xenograft models of pediatric brain tumors alone and in combination with chemo- and radiation therapies

Lin Qi[1,2,6], **Holly Lindsay**[1], **Mari Kogiso**[1], **Yuchen Du**[1,2], **Frank K. Braun**[1], **Huiyuan Zhang**[1], **Lei Guo**[3], **Sibo Zhao**[1], **Sarah G. Injac**[1], **Patricia A. Baxter**[1], **Jack MF. Su**[1], **Sophie Xiao**[2], **Stephen W. Erickson**[4], **Eric J. Earley**[4], **Beverly Teicher**[5], **Malcolm A. Smith**[5], **Xiao-Nan Li**[1,2]

[1]Texas Children's Cancer Center, Texas Children's Hospital, Baylor College of Medicine, Houston, TX, USA.

[2]Ann & Robert H. Lurie Children's Hospital of Chicago, Northwestern University Feinberg School of Medicine, Chicago, IL, USA.

[3]Institute of Biosciences and Technology, Texas A&M Health Science Center, Houston, TX, USA.

[4]RTI International, Research Triangle Park, NC, USA.

[5]National Cancer Institute, Bethesda, MD, USA.

[6]Present address: Department of Pharmacology, School of Medicine, Sun Yat-Sen University, Shenzhen 518107, China.

Abstract

Brain tumors are the leading cause of cancer-related death in children. Tazemetostat is an FDA-approved enhancer of zeste homolog (EZH2) inhibitor. To determine its role in difficult-to-treat pediatric brain tumors, we examined EZH2 levels in a panel of 22 PDOX models and confirmed EZH2 mRNA over-expression in 9 GBM (34.6 ± 12.7-fold) and 11 medulloblastoma models (6.2 ± 1.7 in group 3, 6.0 ± 2.4 in group 4) accompanied by elevated H3K27me3 expression. Therapeutic efficacy was evaluated in 4 models (1 GBM, 2 medulloblastomas and 1 ATRT) via systematically administered tazemetostat (250 and 400 mg/kg, gavaged, twice daily) alone and in combination with cisplatin (5 mg/kg, i.p., twice) and/or radiation (2 Gy/day × 5 days).

Reprints and permission information is available at http://www.nature.com/reprints

Correspondence and requests for materials should be addressed to Xiao-Nan Li. xiaonan.li@northwestern.edu.

AUTHOR CONTRIBUTIONS

X.N.L., M.S., and B.T. conceived the project, X.N.L. and M.S. led the experimental design, L.Q., H.L., M.K., Y.D., F.B., H.Z., S.X., S.Z., S.I., P.B., J.M.S., S.X., X.N.L. performed the in vivo studies and immunohistochemical staining, L.Q., Y.D., F.B. led the molecular sub-classification of PDOX models, L.G. and H.Z. performed the Western hybridization, S.W.E., E.J.E. performed the statistical analysis. X.N.L. and L.Q. wrote the manuscript and all authors reviewed the manuscript.

COMPETING INTERESTS

The authors declare no competing interests.

ETHICS APPROVAL/CONSENT TO PARTICIPATE

The patient tumor tissues were collected following our Institutional Review Board (IRB) approved protocols after obtaining consent from the parent(s) or legal guardian (s) of the childhood patients. All the animal experiments were conducted following Institutional Animal Care and Use Committee (IACUC) approved protocols.

Supplementary information The online version contains supplementary material available at https://doi.org/10.1038/s41374-021-00700-8.

Author Manuscript Author Manuscript Author Manuscript Author Manuscript

Compared with the untreated controls, tazemetostat significantly ($P_{corrected} < 0.05$) prolonged survival times in IC-L1115ATRT (101% at 400 mg/kg) and IC-2305GBM (32% at 250 mg/kg, 45% at 400 mg/kg) in a dose-dependent manner. The addition of tazemetostat with radiation was evaluated in 3 models, with only one [IC-1078MB (group 4)] showing a substantial, though not statistically significant, prolongation in survival compared to radiation treatment alone. Combining tazemetostat (250 mg/kg) with cisplatin was not superior to cisplatin alone in any model. Analysis of in vivo drug resistance detected predominance of EZH2-negative cells in the remnant PDOX tumors accompanied by decreased H3K27me2 and H3K27me3 expressions. These data supported the use of tazemetostat in a subset of pediatric brain tumors and suggests that EZH2-negative tumor cells may have caused therapy resistance and should be prioritized for the search of new therapeutic targets.

INTRODUCTION

Brain tumors are the leading cause of cancer-related deaths in children. Despite aggressive treatment with surgery, radiation (XRT), and chemotherapy, the 5-year survival rates remain suboptimal at 60–70% in children with group 3 or 4 medulloblastoma (MB), although >70% in children with non-metastatic group 4 MBs, and drop to <10% after relapse[1-4]. Similarly, the clinical outcome for pediatric glioblastoma (pGBM) and atypical teratoid/rhabdoid tumor (ATRT) are poor as well[5,6]. While analysis of gene mutations[7-13] has provided new hope for expedited translation of target therapies into clinical application, there remain frustrating challenges in translating personalized genomic analysis into effective therapies for pediatric brain tumors. Unlike adult cancers, pediatric brain tumors (MB and GBM) have fewer mutated genes and very scarce recurrent mutations that are druggable “driver/survival-critical mutations”[14], although ATRT is defined by inactivation of the SMARCB1 tumor suppressor gene. Such “silent” mutation profiles make it difficult to develop mutation-targeted therapies. New therapeutic target(s) and alternative novel strategies are needed.

Enhancer of zeste homolog (EZH2) represents an attractive target for brain tumors. EZH2 is the catalytic subunit of polycomb repressive complex 2, a 3-component protein complex which catalyzes the trimethylation of histone 3 at lysine 27 (H3K27). H3K27 trimethylation causes epigenetic silencing of target gene transcription, including genes that regulate cellular proliferation, differentiation, and self-renewal[15-26]. Elevation of EZH2 expression occurs in numerous cancers and correlates with chemotherapy resistance, tumor aggressiveness, and poor prognosis[11,15-23,25,27,28]. Similarly, overexpression of EZH2 has been observed in multiple pediatric brain tumors. Group 3 and 4 MBs are shown to express high levels of EZH2[7-9,29], whereas in ATRTs the absence of SMARCB1 protein is well documented to promote higher EZH2 repressive activity and dependence. In H3K27M-mutant pediatric gliomas, EZH2 has been identified as a potential therapeutic target[30]. Aberrant EZH2 activities result in increased H3K27 trimethylation (H3K27me3) and consequently decrease tumor suppressor gene expression and promoting tumorigenesis[29]. Targeting EZH2 has led to strong anti-tumor activities. Indeed, multiple EZH2 inhibitors have been developed[31]. Tazemetostat is an orally available EZH2 inhibitor that has entered clinical trials both in pediatric and adult patients. It has exhibited activities in adult cancers with SMARCB1 loss[32] and is recently approved by FDA for patients with epithelioid sarcoma and relapsed/

Author Manuscript Author Manuscript Author Manuscript Author Manuscript

refractory follicular lymphoma (FL)[33]. However, its capacity in passing through the blood brain barrier and in targeting pediatric brain tumors remains incompletely understood.

In vivo examination of therapeutic efficacy of new treatments is often delayed by the lack of clinically relevant and molecularly accurate animal models. To overcome this barrier, we directly implanted patient tumor specimens into the matching locations in the brains of SCID mice and established a panel of patient-derived orthotopic xenograft (PDOX) mouse models, including group 3 and 4 MBs, pGBMs, and ATRT. These models were shown to have replicated the histology, invasion/metastasis and preserved major genetic abnormalities of the original patient tumors[34-36]. They have thus provided a useful platform for the preclinical drug testing of new therapeutic modalities[37,38]. Since all the xenografts were implanted in mouse brains, these models can also help determine if investigational drug(s) can be effectively delivered into orthotopic xenografts.

In this study, we examined the expression of EZH2 in a panel of 22 PDOX mouse models of pediatric MBs, GBMs and an ATRT. We analyzed the levels of H3K27me3 in tumor tissue to better understand the potential of EZH2 as a therapeutic target and then analyzed the anti-tumor activities of the EZH2 inhibitor tazemetostat in vivo in PDOX models. Recognizing the limitations of single agent and intra-tumoral heterogeneity, we further examined if combining tazemetostat with fractionated radiation and/or clinically relevant chemotherapies, which are part of the standard of care, would further improve animal survival times in PDOX models of different pediatric brain tumors. The mechanisms of therapy resistance were subsequently analyzed in the recurrent/remnant tumors of the treated PDOX models. Our aim is to provide detailed preclinical evidence to support the use of EZH2 inhibitors in childhood malignant brain tumors.

MATERIALS AND METHODS

EZH2 inhibitor

Tazemetostat was supplied by Epizyme (Cambridge, MA). It is a potent and selective EZH2 inhibitor (MW 572.74) with Ki and IC_{50} of 2.5 nM and 11 nM in cell free-assays, respectively.

PDOX mouse models

SCID mice, (NOD.129S7(B6) -Rag1^{tm1Mom}/J, Stock No: 003729, Jackson Laboratories), 5–8 weeks of both male and female were house and breed in the animal facility of Texas Children’s Hospital and Lurie Children’s Hospital animal facility. This strain of mice is radiation-resistant and can tolerate fractionated radiation therapy as we described previously[39]. All the animal experiments were performed following Institutional Animal Care and Use Committee (IACUC) approved protocols. A total of 22 PDOX mouse models were developed and characterized as we described previously[34,35,37-40]. Nineteen models were established from freshly resected brain tumor specimens collected from patients after the signed informed consent obtained prior to sample acquisition in accordance with our local Institutional Review Board approved protocol. Three additional models (2 DIPGs and

Author Manuscript Author Manuscript Author Manuscript Author Manuscript

1 ATRT) were established from autopsied tumor tissues. All animal experiments with NOD/SCID mice were conducted under an IACUC-approved protocol[34,41].

Immunohistochemistry (IHC)

IHC was performed using a Vectastain Elite kit (AK-5001, Vector Laboratories, Burlingame, CA) as described previously[34,42,43]. Primary antibodies included the human-specific Ki67 (1:50) (Thermo Fisher, Waltham, MA), and rabbit anti-EZH2 (1:50) (Thermo Fisher, Waltham, MA) and H3K27me2 (1:100) (ABCAM INC, Cambridge, CA), and H3K27me3(1:50) (Thermo Fisher, Waltham, MA).

Western hybridization

To analyze the changes of histone methylation, histones were prepared by acid extraction[43]. Primary antibodies (1:1000 dilution) against H3K27me3 were incubated.

In vivo treatment in PDOX models and Statistical analysis

Cryopreserved xenograft tumor cells were injected into the brains of SCID mice as we described previously[34,42]. Tazemetostat was administered through oral gavage, twice daily at 250 and 400 mg/kg on days 14–41 post tumor implantation as single agent or at 250 mg/kg in combination with chemo- or radiation. Fractionated radiation (XRT) was delivered locally at 2 Gy/day × 5 days (on days 21–25), and Cisplatin was given at 5 mg/kg, i.p., once daily on day 21 and 24 post tumor implantation. For ATRT and GBM models, 50 mice per model were divided into five groups ($n = 10$ per group), i.e., control, tazemetostat (250 and 400 mg/kg groups), XRT only and tazemetostat 250 mg/kg + XRT. For MB models, 80 mice per model were divided into 8 groups ($n = 10$ per groups), i.e., control, tazemetostat (250 and 400 mg/kg groups), XRT only, Cisplatin only, tazemetostat (250 mg/kg) + XRT, tazemetostat (250 mg/kg) + cisplatin, and tazemetostat (250 mg/kg) + XRT + cisplatin. Differences in event-free survival (EFS) between the treatment groups were analyzed using the Peto and Peto modification of the Gehan-Wilcoxon test. P values were Bonferroni-corrected for multiple testing, based on 4 treatment groups tested with IC-2305GBM and IC-L1115ATRT and 7 treatment groups tested with ICb-1078MB and ICb-1572MB, except where ad hoc pairwise comparisons between treatment groups are denoted P_{nominal}.

RESULTS

EZH2 is overexpressed in pediatric brain tumors

The expression levels of EZH2 mRNA of PDOX and matching patient tumors were extracted from gene expression profiling data completed with Affymetric U133 arrays. To further evaluate the generalizability of our data from brain tumors to other types of pediatric cancers, we also extracted RNAseq data from a panel of >270 xenograft tumors of pediatric cancers assembled by the NIH/NCI Pediatric Preclinical Testing Consortium (PPTC)[36]. High levels of EZH2 mRNA expression were detected in a majority of the pediatric cancers, including leukemia, sarcomas, neuroblastoma, and various types of brain tumors (Fig. 1). To identify brain tumor models that replicate EZH2 overexpression and to determine if the preservation of EZH2 expression status was broadly recapitulated in

Author Manuscript Author Manuscript Author Manuscript Author Manuscript

multiple PDOX models during serial subtransplantations, we examined the changes of EZH2 expression in a set of 22 PDOX models of pediatric brain tumors and directly compared with their matching patient tumors. Remarkably increased (>10 fold as compared with normal childhood cerebral tissues) EZH2 mRNA expression was detected in 9/9 pGBM models and medium level (>2 fold but <10 fold) were detected in 2/2 DIPG models (Fig. 2A). When compared with the original patient tumors, the matching PDOX tumors expressed similar ($n = 1$) or higher ($n = 6$) levels of EZH2 mRNA that were maintained during serial in vivo subtransplantations in mouse brains. Similarly, elevated EZH2 mRNA (~2–10 fold) were detected in 11 MB PDOX models that represented group 3 ($n = 4$), group 4 ($n = 3$), SHH ($n = 2$) and WNT ($n = 2$) when compared with the childhood normal cerebral and cerebellar tissues. The increased EZH2 mRNA expression was maintained during PDOX tumor serial subtransplantations (from passage I to V) and slightly higher than the matching patient tumors ($n = 9$) (Fig. 2B). Protein expression of H3K27me3, which is frequently increased in tumors with aberrant activation of EZH2, was examined in MB PDOX tumors although its expression status has not been well examined in GBMs (outside brain stem), MB and ATRT tumors. Immunohistochemical staining showed strong (+++) to medium (++) positivity in the nuclei of tumor cells in both group 3 and 4 MB xenograft tumors (Fig. 2C). When compared with three normal childhood cerebellar tissues that expressed low/no H3K27me3, the MB xenografts (3/3 group 3 and 3/4 group 4) expressed high levels of H3K27me3 (Fig. 2D). These findings identified a panel of PDOX models bearing the activated EZH2 gene.

Targeting EZH2 with tazemetostat acting alone and in combination with chemotherapy and/or radiation therapy

The therapeutic efficacy of EZH2 inhibitor tazemetostat[32,44] was examined in PDOX models, including one ATRT, one pGBM and two MBs, that expressed high levels of EZH2 mRNA (Table 1). All the xenograft tumors were implanted into the matching locations in the mouse brains, i.e., supra-tentorial ATRT and pGBM to mouse cerebra (intra-cerebral, IC), and MBs to mouse cerebellar (intracerebellar, ICb) with identical cell numbers (1×10^5 cells/mouse). To determine the dose effects, two doses of tazemetostat, 250 and 400 mg/kg, were gavaged twice daily from day 14-41 (total 28 days) post tumor cell implantation. To determine the efficacy of combination therapy, low dose of tazemetostat (250 mg/kg) was selected to combine with fractionated radiations to avoid excessive toxicity potentially associated with the high dose (400 mg/kg). Changes of body weight were used as surrogate marker of therapy-related toxicities.

The ATRT model, IC-L1115ATRT, was derived from an autopsied supratentorial ATRT with confirmed SMARCB1 deletion. Treatment with tazemetostat (Fig. 3A) for 28 days at 250 mg/kg increased the median animal survival times from 70.5 days in the control group to 98 days, but the difference was not significant ($P_{\text{corrected}} = 0.927$). Increasing the dose to 400 mg/kg, however, significantly prolonged the animal survival times to 141.5 days ($P_{\text{corrected}} = 0.024$). Combining tazemetostat (250 mg/kg) with chemotherapy agent cisplatin (5 mg/kg, once daily, *i.p.*, on day 21 and 24) increased animal survival times to 142.5 days ($P_{\text{corrected}} = 0.003$ vs. control) which was actually shorter than mice treated with cisplatin alone (150 days, $P_{\text{nominal}} = 0.272$ between treatment groups), revealing no therapeutic enhancement from the combination (Supplemental Table 1).

Author Manuscript Author Manuscript Author Manuscript Author Manuscript

The pGBM model, IC-2305GBM, expressed high levels (>20 folds) of EZH2 mRNA (Fig. 2A). When treated with tazemetostat as single agent at 250 mg/kg, the median animal survival times extended from 46 days in the control group to 60.5 days ($P_{corrected}$ = 0.004) (Fig. 3B); increasing the dose to 400 mg/kg further prolonged the survival times to 66.5 days ($P_{corrected}$ = 0.001), exhibiting a dose-dependent therapeutic efficacy. Fractionated radiation (2 Gy/day for 5 days starting from day 14) was active as well, extending animal survival times to 77.5 days ($P_{corrected}$ = 0.004). Combining tazemetostat with radiation, however, did not further increase survival times beyond those achieved by tazemetostat or radiation acting alone, indicating a lack of additive or synergistic activities (Supplemental table 1).

Two MB models, ICb-1572MB (group 3) and ICb-1078MB (group 4), with elevated EZH2 mRNA (5–6 fold) and protein expression were selected for a combinatory treatment regimen. For each model, 80 mice were implanted with PDOX cells (completed within 2 h) and divided into 8 groups (n = 10), including control, 4 single agent groups (tazemetostat at 250 mg/kg and 400 mg/kg, cisplatin at 5 mg/kg, radiation 2 Gy/day × 5 days), two drug-combination (tazemetostat at 250 mg/kg + XRT, tazemetostat at 250 mg/kg + cisplatin), and three drug combination (tazemetostat at 250 mg/kg + XRT + cisplatin) (Supplemental Table 1). In the group 3 MB model, ICb-1572MB (Fig. 3C), only treatment with tazemetostat + XRT + cisplatin significantly prolonged survival time ($P_{corrected}$ = 0.026) from 25 to 32 days. However, without a separate treatment group of XRT + cisplatin, the contribution of tazemetostat cannot be ascertained. In the group 4 MB model, IC-1078MB (Fig. 3D), tazemetostat at 250 mg/kg alone was able to prolong the median animal survival times from 49.5 days to 68.5 days (38% increase, $P_{corrected}$ = 0.010 vs. control), while the higher dose at 400 mg/kg resulted in a shorter survival time of 60 days ($P_{corrected}$ = 0.282). XRT as a single treatment, however, prolonged animal survival times to 77 days ($P_{corrected}$ = 0.015 vs. control). Combining the two active single treatments, tazemetostat (250 mg/kg) and XRT (2 Gy/day × 5 day), more than doubled (118% increase) the animal survival times to 108 days ($P_{corrected}$ = 0.010 vs. tazemetostat, $P_{corrected}$ = 0.028 vs. radiation alone). The chemotherapy agent, cisplatin, was not able to cause significant improvement of animal survival time as single agent (70.5 days, $P_{corrected}$ = 1.000) nor in combination with tazemetostat (250 mg/kg) (67.5 days, $P_{corrected}$ = 1.000). Adding cisplatin to the tazemetostat + XRT combination did not enhance the anti-tumor activities but reduced survival time from 108 days to 76 days (Supplemental Table 1). In summary, tazemetostat at 250 mg/kg was active in one of the two MB models as single agent and combination with fractionated radiation prolonged animal survival times;increasing tazemetostat dose to 400 mg/kg did not improve therapeutic efficacy;cisplatin was not active either as a single agent or in combination with other agents.

Histological changes induced by tazemetostat

Despite significant extension of animal survival time, all the treated mice died. Histological analysis of whole mouse brains following in vivo treatment (Fig. 4A) often revealed large orthotopic PDX tumors (Fig. 4B, C). Overall growth pattern was similar between the control and the treated mice. Although EZH2 inhibitors were postulated to suppress tumor invasion[19], our detailed histological analysis of whole mouse brains did not find major suppressions in IC-L1115ATRT (although the number of invasive satellite foci was slightly

Author Manuscript Author Manuscript Author Manuscript Author Manuscript

decreased) (Fig. 4B) nor in the ICb-1078MB (Fig. 4C). Compared with the untreated groups, the remnant tumors exhibited similar levels of cell proliferation as detected by Ki-67 (Fig. 4B, C). Altogether, these data suggested that the recurrent tumors maintained histological features after tazemetostat treatment.

Assess the underlying biological changes mediating the resistance of EZH2 inhibition

Since previous studies have examined extensively the mechanism of EZH2 inhibition induced cell killing[20,25,27-30], we focused on the mechanism of tumor resistance. We first examined the molecular target EZH2 in the remnant PDOX tumors in a responsive ATRT model (IC-L1115) and a MB model that was less responsive to tazemetostat acting alone (ICb-1078MB). We did not attempt to analyze the remaining two models, because ICb-1572MB was not responsive to any treatments; and IC-2305GBM was less responsive than XRT acting alone and combining tazemetostat with XRT resulted in reduced animal survival times. In IC-L1115ATRT remnant tumors ($n = 3$), the overall expression of EZH2 was remarkably reduced both in the tumor mass and in the invasive front (Fig. 5A). There was a noticeable increase of EZH2 negative cells (Fig. 5A) with occasional formation of large circular areas of low cell density pouches distinct from the surrounding EZH2 positive cells (Supplemental Fig. 1). In ICb-1078MB remnant tumors, the overall levels of EZH2 protein expression were reduced from high (+++) to low or medium (+ ~++), and EZH2 negative cells increased from <1% in the untreated tumor to 5-10% (Fig. 5B). These data suggested that many of the tumor cells with strong (+++) EZH2 cells were eliminated, and it was the tumor cells with no or reduced EZH2 expression that survived and repopulated tumor formation.

As the mechanism of action for EZH2 inhibitors is through EZH2 inhibition with passive removal of the H3K27 methyl mark by histone turnover, we next examined the changes of H3K27 both as bi- and tri-methylations (H3K27me2 and H3K27me3). In IC-L1115ATRT, tumor cells positive for H3K27me2 and H3K27me3 were reduced from medium (++) to low (+) and from strong (+++) to medium (++), respectively. Similar trends were found both in the tumor core and in the invasive front (Fig. 5A). In IC-1078MB, the changes of H3K27me2 and H3K27me3 were less prominent as their levels in the untreated control tumors were low to medium (+~++) (Fig. 5B), much lower than that in the ARTR model. These data indicated that the changes of H3K27me2 and H3K27me3 were consistent with EZH2 suppression, particularly in the ATRT model.

DISCUSSION

Tazemetostat is an EZH2 inhibitor that is approved by FDA for patients aged 16 years and older with metastatic or locally advanced epithelioid sarcoma not eligible for complete resection. It is also approved for adult patients with relapsed or refractory (R/R) FL whose tumors are positive for an EZH2 mutation as detected by an FDA-approved test and who have received at least 2 prior systemic therapies, and for adult patients with R/R FL who have no satisfactory alternative treatment options. Clinical trials in children with cancer have been initiated[45]. Given the genomic and epigenetic complexity of cancer, a single therapeutic agent may show some degree of activity, but optimal therapeutic benefit may be

Author Manuscript Author Manuscript Author Manuscript Author Manuscript

found in combination with other active agents. To provide preclinical evidence to support its use in pediatric brain tumors, we utilized 4 PDOX models of three different diagnoses and designed a strategy to test single agent (at different doses) and comprehensive combinations with radiation and/or chemotherapy.

Identifying EZH2 as a therapeutic target is the first step for the development of new therapies. EZH2 expression have been detected and correlates with chemotherapy resistance, tumor aggressiveness, and poor prognosis[11,15,17-23,27,28]. Similar to these findings, we showed that the over-expressed EZH2 in the original patient tumors of MB and high grade glioma was well preserved in the matching PDOX models even during serial in vivo subtransplantations. This set of data is important not only to confirm the molecular fidelity of PDOX models but also to provide a key set of model system to support the preclinical drug testing of EZH2 inhibitors. However, the EZH2 expression in our ATRT model was not significantly elevated and past work by the Pediatric Preclinical Testing Program showed that tazemetostat was effective only for rhabdoid tumors and not for other pediatric solid tumors[46]. Therefore, caution has to be exercised when using EZH2 over-expression as sole indicator of tumor selection, particularly as clinical activity of tazemetostat (outside of lymphomas) has been observed almost exclusively in patients with genomic alterations leading to SMARCB1 (or SMARCA4) loss.

Treatment with tazemetostat as a single agent significantly prolonged animal survival times in an ATRT model (IC-L1115ATRT) and a GBM model (IC-2305GBM) in a dose-dependent manner, and in a MB model (ICb-1078MB) at low (250 mg/kg) dose. Radiation therapy significantly ($P < 0.05$) prolonged survival time for 2/3 models tested (IC-2305GBM and ICb-1078MB, but not ICb-1572MB). Cisplatin as a single agent significantly prolonged survival for only L115ATRT, but not for either of the MB models. Analysis of combination therapies of tazemetostat (at 250 mg/kg) with clinically-relevant fractionated radiation therapies in three PDOX models identified the group 4 MB ICb-1078MB as the one that exhibited extension of animal survival times compared to the radiation-alone group (40% increase), though statistical significance was not achieved. For both IC-2305GBM and IC-L115ATRT, the addition of tazemetostat to radiation was without benefit. The addition of tazemetostat to cisplatin did not improve survival compared to single agent cisplatin for any of the three models studied (two MB and one ATRT). While the triple therapy (tazemetostat and radiation and cisplatin) significantly prolonged survival in comparison to the control group, it was not superior to the doublet combinations. Although the 4 models shared high-level expression of EZH2 mRNA, they each carried additional and different genetic abnormalities. Such heterogeneities may have played a role in the differential responses of these models and should be taken into consideration in future experimental design of preclinical drug testing.

Combining novel targeted therapy with existing standard of care treatments has the advantage of rapid integration into clinical applications. However, to establish an in vivo treatment protocol of complex combination therapies that can be safely administered to animal models is still a challenge. In the field of brain tumors, standard therapy typically involves the use of radiation. Unfortunately, most strains of SCID mice (immunocompromised animals) involved in orthotopic xenograft model development are

Author Manuscript Author Manuscript Author Manuscript Author Manuscript

unable to tolerate radiation. After a search of the available literature and experimental testing[39], we confirmed that the SCID mice, (NOD.129S7(B6) -Rag1^{tm1Mom}/J, Stock No: 003729, https://www.jax.org/strain/003729), can tolerate fractionated radiation therapy very well, thereby providing an important host animal resource for testing radiation therapies in brain tumors. Our successful completion of the complex combination (tazemetostat + fractionated radiation and/or chemotherapy) treatment in the four PDOX models without serious toxicities also established the feasibility and supports future examination of multi-drug combinations.

Many efforts have been made to understand the mechanisms of action of tazemetostat[47-49]. Since all our treated mice eventually died of disease, we analyzed the remnant/recurrent tumors to understand the potential mechanisms of resistance/relapse. While we did not find major differences in tumor growth pattern, invasion and cell proliferation before and after tazemetostat treatment, our analysis of the remnant tumors revealed remarkable increase of the tumor cells with no or low EZH2 expression and reduced levels of H3K27me2 an H3K27me3. Since such cells were initially present in the untreated PDOX cells at very low abundance, this finding suggested that intra-tumoral heterogeneity need to be carefully addressed in future. Recent advancement of single cell sequencing[50] and spatial single cell analysis should provide a novel technology to facilitate the understanding of drug resistance at the single cell level.

In summary, we demonstrated that EZH2 overexpression is present in pediatric cancers and well preserved in a panel of PDOX models of brain tumors. The FDA-approved EZH2 inhibitor, tazemetostat, prolongs survival in an ATRT and a GBM model when acting alone and exhibited a trend to increase XRT efficacy in a group 4 MB, although combination with cisplatin did not improve animal survival times. Although overexpression of EZH2 has been frequently detected in multiple human cancers, our data suggested tumors with EZH2 over-expression, particularly examined from bulk tissues, do not always respond to EZH2 inhibitor. The inter-tumoral heterogeneity, particularly the cell with low or no EZH2 expression, may have caused the tumor recurrence in the current study. Our data support the evaluation of tazemetostat in a subset of pediatric brain tumors.

Supplementary Material

Refer to Web version on PubMed Central for supplementary material.

ACKNOWLEDGEMENTS

The authors wish to thank all the veterinarians and veterinary technicians of the Center of Comparative Medicine in Baylor College of Medicine and staff members of the Feigin Center animal facility at Texas Children's Hospital for their excellent support of our animal experiments.

FUNDING

This work was funded by NIH/NCI grants RO1 CA185402 (X.N.L.), U01 CA217613 (X.N.L.), and U0 1 CA199222.

Author Manuscript Author Manuscript Author Manuscript Author Manuscript

DATA AVAILABILITY

Data are either presented in the manuscript or provided in the supplemental figures/tables.

REFERENCES

1. Northcott PA et al. Medulloblastoma comprises four distinct molecular variants. J. Clin. Oncol 29, 1408–1414 (2011). [PubMed: 20823417]
2. Taylor MD et al. Molecular subgroups of medulloblastoma: the current consensus. Acta Neuropathol. 123, 465–472 (2012). [PubMed: 22134537]
3. Ramaswamy V & Taylor MD Medulloblastoma: from myth to molecular. J. Clin. Oncol 35, 2355–2363 (2017). [PubMed: 28640708]
4. Sabel M et al. Relapse patterns and outcome after relapse in standard risk medulloblastoma: a report from the HIT-SIOP-PNET4 study. J. Neurooncol 129, 515–524 (2016). [PubMed: 27423645]
5. Espinoza JC et al. Outcome of young children with high-grade glioma treated with irradiation-avoiding intensive chemotherapy regimens: final report of the Head Start II and III trials. Pediatr. Blood Cancer 63, 1806–1813 (2016). [PubMed: 27332770]
6. Jones C et al. Pediatric high-grade glioma: biologically and clinically in need of new thinking. Neuro Oncol. 19, 153–161 (2017). [PubMed: 27282398]
7. Batora NV et al. Transitioning from genotypes to epigenotypes: why the time has come for medulloblastoma epigenomics. Neuroscience 264, 171–185 (2014). [PubMed: 23876321]
8. Dubuc AM et al. Aberrant patterns of H3K4 and H3K27 histone lysine methylation occur across subgroups in medulloblastoma. Acta Neuropathol. 125, 373–384 (2013). [PubMed: 23184418]
9. Jones DT, Northcott PA, Kool M & Pfister SM The role of chromatin remodeling in medulloblastoma. Brain Pathol. 23, 193–199 (2013). [PubMed: 23432644]
10. Parsons DW et al. The genetic landscape of the childhood cancer medulloblastoma. Science 331, 435–439 (2011). [PubMed: 21163964]
11. Bender S et al. Reduced H3K27me3 and DNA hypomethylation are major drivers of gene expression in K27M mutant pediatric high-grade gliomas. Cancer Cell 24, 660–672 (2013). [PubMed: 24183680]
12. Schwartzentruber J et al. Driver mutations in histone H3.3 and chromatin remodelling genes in paediatric glioblastoma. Nature 482, 226–231 (2012). [PubMed: 22286061]
13. Sturm D et al. Hotspot mutations in H3F3A and IDH1 define distinct epigenetic and biological subgroups of glioblastoma. Cancer Cell 22, 425–437 (2012). [PubMed: 23079654]
14. Eifert C & Powers RS From cancer genomes to oncogenic drivers, tumour dependencies and therapeutic targets. Nat. Rev. Cancer 12, 572–578 (2012). [PubMed: 22739505]
15. Wilson BG et al. Epigenetic antagonism between polycomb and SWI/SNF complexes during oncogenic transformation. Cancer Cell 18, 316–328 (2010). [PubMed: 20951942]
16. Fiskus W et al. Combined epigenetic therapy with the histone methyltransferase EZH2 inhibitor 3-deazaneplanocin A and the histone deacetylase inhibitor panobinostat against human AML cells. Blood 114, 2733–2743 (2009). [PubMed: 19638619]
17. Yoo KH & Hennighausen L EZH2 methyltransferase and H3K27 methylation in breast cancer. Int. J. Biol. Sci 8, 59–65 (2012). [PubMed: 22211105]
18. Chiba T et al. 3-Deazaneplanocin A is a promising therapeutic agent for the eradication of tumor-initiating hepatocellular carcinoma cells. Int. J. Cancer 130, 2557–2567 (2012). [PubMed: 21717453]
19. Crea F et al. EZH2 inhibition: targeting the crossroad of tumor invasion and angiogenesis. Cancer Metastasis Rev. 31, 753–761 (2012). [PubMed: 22711031]
20. Chase A & Cross NC Aberrations of EZH2 in cancer. Clin. Cancer Res 17, 2613–2618 (2011). [PubMed: 21367748]
21. Knutson SK et al. Durable tumor regression in genetically altered malignant rhabdoid tumors by inhibition of methyltransferase EZH2. Proc. Natl Acad. Sci. USA 110, 7922–7927 (2013). [PubMed: 23620515]

Author Manuscript Author Manuscript Author Manuscript Author Manuscript

22. Alimova I et al. Inhibition of EZH2 suppresses self-renewal and induces radiation sensitivity in atypical rhabdoid teratoid tumor cells. Neuro Oncol. 15, 149–160 (2013). [PubMed: 23190500]
23. Ezponda T & Licht JD Molecular pathways: deregulation of histone H3 lysine 27 methylation in cancer-different paths, same destination. Clin. Cancer Res 10.1158/1078-0432.CCR-13-2499 (2014).
24. Venneti S et al. Evaluation of histone 3 lysine 27 trimethylation (H3K27me3) and enhancer of Zest 2 (EZH2) in pediatric glial and glioneuronal tumors shows decreased H3K27me3 in H3F3A K27M mutant glioblastomas. Brain Pathol. 23, 558–564 (2013). [PubMed: 23414300]
25. Suva ML et al. EZH2 is essential for glioblastoma cancer stem cell maintenance. Cancer Res. 69, 9211–9218 (2009). [PubMed: 19934320]
26. Sun Y, Bailey CP, Sadighi Z, Zaky W & Chandra J Pediatric high-grade glioma: aberrant epigenetics and kinase signaling define emerging therapeutic opportunities. J. Neurooncol 150, 17–26 (2020). [PubMed: 32504402]
27. McCabe MT et al. EZH2 inhibition as a therapeutic strategy for lymphoma with EZH2-activating mutations. Nature 492, 108–112 (2012). [PubMed: 23051747]
28. Fan TY et al. Inhibition of EZH2 reverses chemotherapeutic drug TMZ chemosensitivity in glioblastoma. Int. J. Clin. Exp Pathol 7, 6662–6670 (2014). [PubMed: 25400745]
29. Alimova I et al. Targeting the enhancer of zeste homologue 2 in medulloblastoma. Int. J. Cancer 131, 9 (2012).
30. Mohammad F et al. EZH2 is a potential therapeutic target for H3K27M-mutant pediatric gliomas. Nat. Med 23, 483–492 (2017). [PubMed: 28263309]
31. Kim KH & Roberts CW Targeting EZH2 in cancer. Nat. Med 22, 128–134 (2016). [PubMed: 26845405]
32. Gounder M et al. A phase II, multicenter study of the EZH2 inhibitor tazemetostat in adults: Epithelioid sarcoma cohort (NCT02601950). Ann. Oncol 29, viii581–viii582 (2018).
33. First EZH2 inhibitor approved-for rare sarcoma. Cancer Discov. 10, 333–334 (2020). [PubMed: 32041739]
34. Shu Q et al. Direct orthotopic transplantation of fresh surgical specimen preserves CD133+ tumor cells in clinically relevant mouse models of medulloblastoma and glioma. Stem Cells 26, 1414–1424 (2008). [PubMed: 18403755]
35. Zhao X et al. Global gene expression profiling confirms the molecular fidelity of primary tumor-based orthotopic xenograft mouse models of medulloblastoma. Neuro. Oncol 14, 574–583 (2012). [PubMed: 22459127]
36. Rokita JL et al. Genomic profiling of childhood tumor patient-derived xenograft models to enable rational clinical trial design. Cell Rep. 29, 1675–1689.e1679 (2019). [PubMed: 31693904]
37. Liu Z et al. Intravenous injection of oncolytic picornavirus SVV-001 prolongs animal survival in a panel of primary tumor-based orthotopic xenograft mouse models of pediatric glioma. Neuro Oncol. 15, 1173–1185 (2013). [PubMed: 23658322]
38. Yu L et al. A single intravenous injection of oncolytic picornavirus SVV-001 eliminates medulloblastomas in primary tumor-based orthotopic xenograft mouse models. Neuro Oncol. 13, 14–27 (2010). [PubMed: 21075780]
39. Huang L et al. Systems biology-based drug repositioning identifies digoxin as a potential therapy for groups 3 and 4 medulloblastoma. Sci. Transl. Med 10 10.1126/scitranslmed.aat0150 (2018).
40. Grasso CS et al. Functionally defined therapeutic targets in diffuse intrinsic pontine glioma. Nat. Med 21, 555–559 (2015). [PubMed: 25939062]
41. Kogiso M et al. Concurrent Inhibition of Neurosphere and Monolayer Cells of Pediatric Glioblastoma by Aurora A Inhibitor MLN8237 Predicted Survival Extension in PDOX Models. Clin Cancer Res. 24, 2159–2170 (2018). [PubMed: 29463553]
42. Yu L et al. A clinically relevant orthotopic xenograft model of ependymoma that maintains the genomic signature of the primary tumor and preserves cancer stem cells in vivo. Neuro Oncol. 12, 580–594 (2010). [PubMed: 20511191]
43. Shu Q et al. Valproic acid prolongs survival time of severe combined immunodeficient mice bearing intracerebellar orthotopic medulloblastoma xenografts. Clin. Cancer Res 12, 4687–4694 (2006). [PubMed: 16899619]

Author Manuscript Author Manuscript Author Manuscript Author Manuscript

44. Italiano A et al. Tazemetostat, an EZH2 inhibitor, in relapsed or refractory B-cell non-Hodgkin lymphoma and advanced solid tumours: a first-in-human, open-label, phase 1 study. Lancet Oncol. 19, 649–659 (2018). [PubMed: 29650362]

45. Chi SN et al. Phase I study of tazemetostat, an enhancer of zeste homolog-2 inhibitor, in pediatric pts with relapsed/refractory integrase interactor 1-negative tumors. J. Clin. Oncol 38, 10525–10525 (2020).

46. Kurmasheva RT et al. Initial testing (stage 1) of tazemetostat (EPZ-6438), a novel EZH2 inhibitor, by the Pediatric Preclinical Testing Program. Pediatr. Blood Cancer 64 10.1002/pbc.26218 (2017).

47. da Hora CC et al. Sustained NF-kappaB-STAT3 signaling promotes resistance to Smac mimetics in Glioma stem-like cells but creates a vulnerability to EZH2 inhibition. Cell Death Discov. 5, 72 (2019). [PubMed: 30854231]

48. Brach D et al. EZH2 inhibition by tazemetostat results in altered dependency on B-cell activation signaling in DLBCL. Mol. Cancer Ther 16, 2586–2597 (2017). [PubMed: 28835384]

49. Erkek S et al. Comprehensive analysis of chromatin states in atypical teratoid/rhabdoid tumor identifies diverging roles for SWI/SNF and polycomb in gene regulation. Cancer Cell 35, 95–110 (2019). e118. [PubMed: 30595504]

50. Hovestadt V et al. Resolving medulloblastoma cellular architecture by single-cell genomics. Nature 572, 74–79 (2019). [PubMed: 31341285]

Author Manuscript Author Manuscript Author Manuscript Author Manuscript

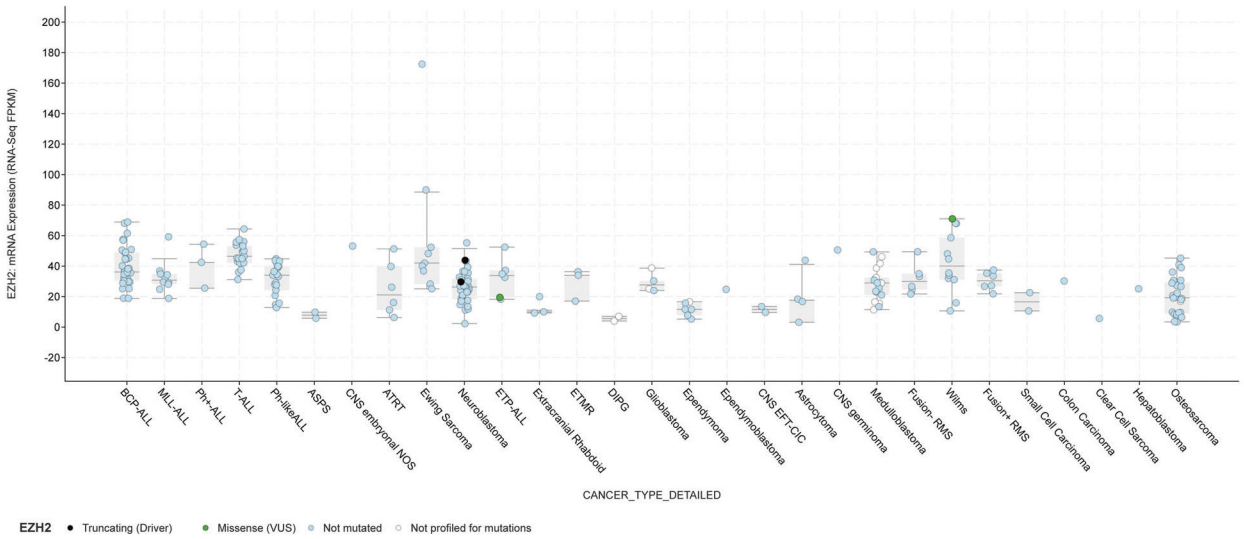

Fig. 1. Expression of EZH2 mRNA in a panel of xenograft mouse models of pediatric cancers.

Data were extracted from RNAseq analysis of PPTC xenograft tumors (see ref. [36]) and presented as FPKM (Fragments Per Kilobase of transcript per Million mapped reads). Models with truncating (black filled circle) or missense (green filled circle) mutations were shown.

Author Manuscript Author Manuscript Author Manuscript Author Manuscript

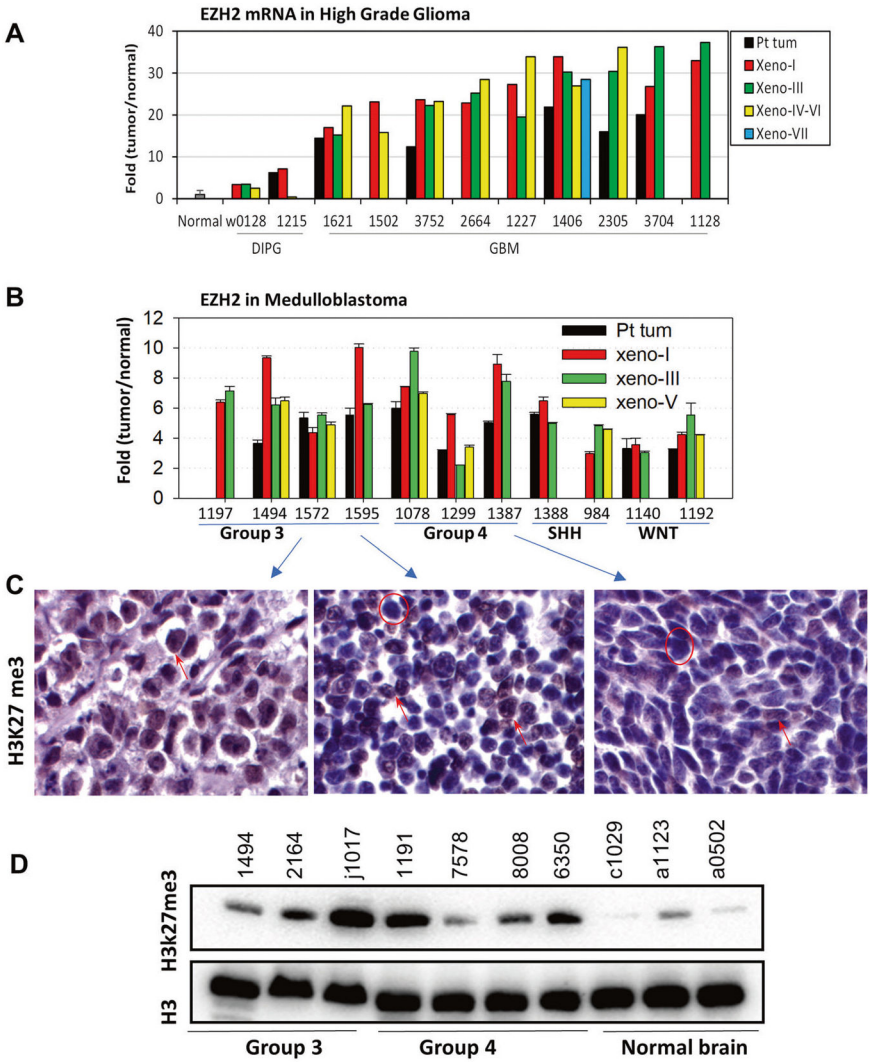

Fig. 2. EZH2 overexpression in pediatric brain tumors.

A, **B**. High levels of EZH2 mRNA expression in high-grade glioma (*upper panel*) and MB (*lower panel*) patient tumors (*Pt tum*) and PDOX models during serial in vivo subtransplantation from passage I (*Xeno-I*) up to passage VIII (*Xeno-VIII*). Normal brain tissues were included as references. The data from glioma were extracted from gene expression profiling using Affy 133 array, and MB from illumine array. **C** Representative immunohistochemical staining images showing increased expression of H3K27me3 in MB models. **D** Western hybridization showing elevated H3K27me3 expression in xenograft tumors of PDOX models. Normal human cerebellar tissues obtained from warm autopsy were included as references.

Author Manuscript Author Manuscript Author Manuscript Author Manuscript

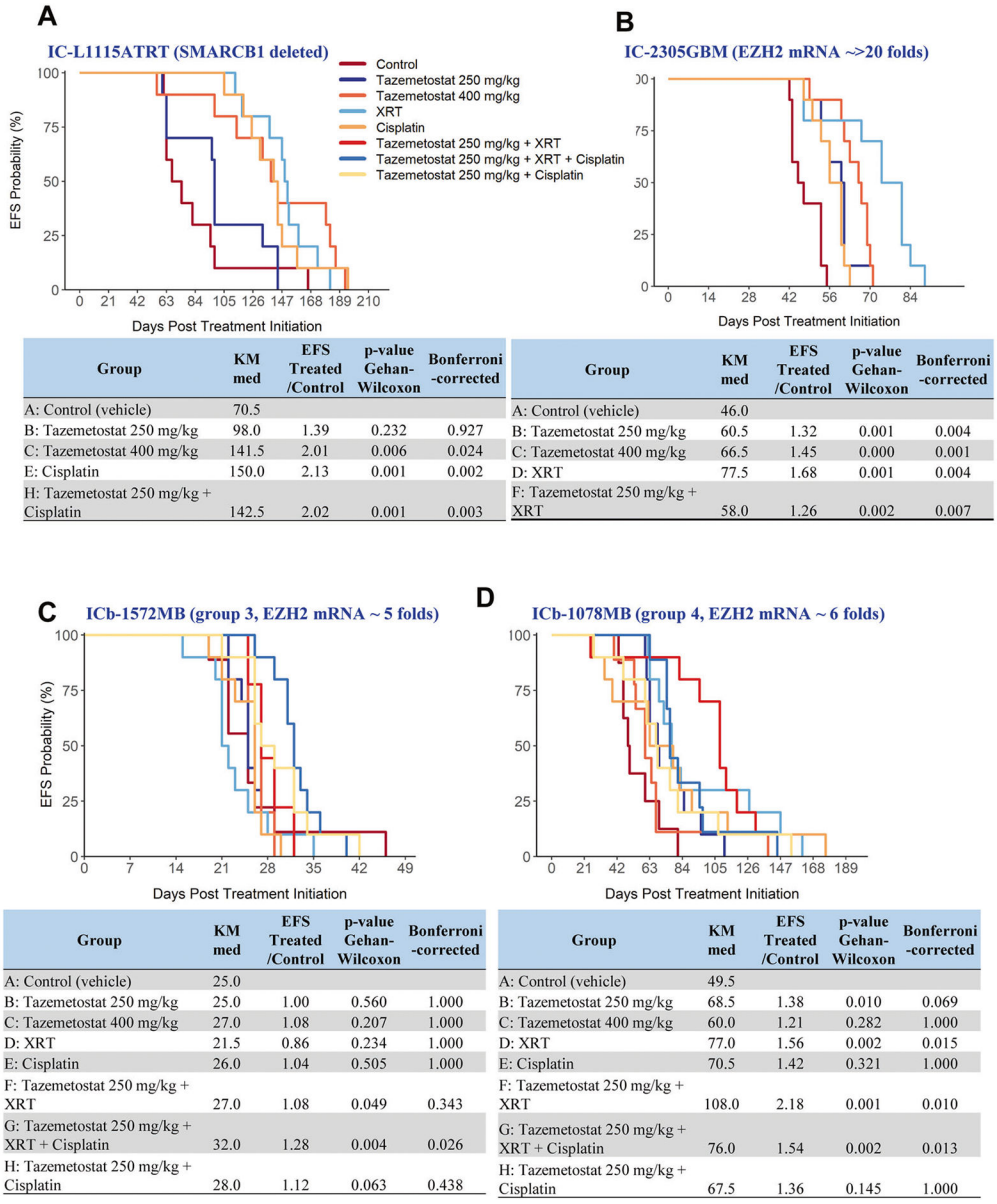

Group	KM med	EFS Treated /Control	p-value Gehan-Wilcoxon	Bonferroni -corrected
A: Control (vehicle)	70.5			
B: Tazemetostat 250 mg/kg	98.0	1.39	0.232	0.927
C: Tazemetostat 400 mg/kg	141.5	2.01	0.006	0.024
E: Cisplatin	150.0	2.13	0.001	0.002
H: Tazemetostat 250 mg/kg + Cisplatin	142.5	2.02	0.001	0.003

Group	KM med	EFS Treated /Control	p-value Gehan-Wilcoxon	Bonferroni -corrected
A: Control (vehicle)	46.0			
B: Tazemetostat 250 mg/kg	60.5	1.32	0.001	0.004
C: Tazemetostat 400 mg/kg	66.5	1.45	0.000	0.001
D: XRT	77.5	1.68	0.001	0.004
F: Tazemetostat 250 mg/kg + XRT	58.0	1.26	0.002	0.007

Group	KM med	EFS Treated /Control	p-value Gehan-Wilcoxon	Bonferroni -corrected
A: Control (vehicle)	25.0			
B: Tazemetostat 250 mg/kg	25.0	1.00	0.560	1.000
C: Tazemetostat 400 mg/kg	27.0	1.08	0.207	1.000
D: XRT	21.5	0.86	0.234	1.000
E: Cisplatin	26.0	1.04	0.505	1.000
F: Tazemetostat 250 mg/kg + XRT	27.0	1.08	0.049	0.343
G: Tazemetostat 250 mg/kg + XRT + Cisplatin	32.0	1.28	0.004	0.026
H: Tazemetostat 250 mg/kg + Cisplatin	28.0	1.12	0.063	0.438

Group	KM med	EFS Treated /Control	p-value Gehan-Wilcoxon	Bonferroni -corrected
A: Control (vehicle)	49.5			
B: Tazemetostat 250 mg/kg	68.5	1.38	0.010	0.069
C: Tazemetostat 400 mg/kg	60.0	1.21	0.282	1.000
D: XRT	77.0	1.56	0.002	0.015
E: Cisplatin	70.5	1.42	0.321	1.000
F: Tazemetostat 250 mg/kg + XRT	108.0	2.18	0.001	0.010
G: Tazemetostat 250 mg/kg + XRT + Cisplatin	76.0	1.54	0.002	0.013
H: Tazemetostat 250 mg/kg + Cisplatin	67.5	1.36	0.145	1.000

Fig. 3. In vivo therapeutic efficacy of tazemetostat in PDOX models of childhood brain tumors.
SCID mice were implanted with xenograft cells from the four models, IC-L1115ATRT (**A**), IC-2305GBM (**B**), group 3 (ICb-1572MB) (**C**) and group 4 (ICb-1078MB) (**D**) MBs, were allowed to grow for 14 days to form solid intra-cerebral (IC) or intra-cerebellar (*ICb*) xenograft tumors before being treated with tazemetostat alone and in combinations with chemo- and/or radiation as highlighted in the figures. Kaplan-Meier estimate of median time-to-event, ratio in median time to event between the treated and control groups (EFS T/C), and EFS p values were calculated and compared between the treatment groups.

Author Manuscript Author Manuscript Author Manuscript Author Manuscript

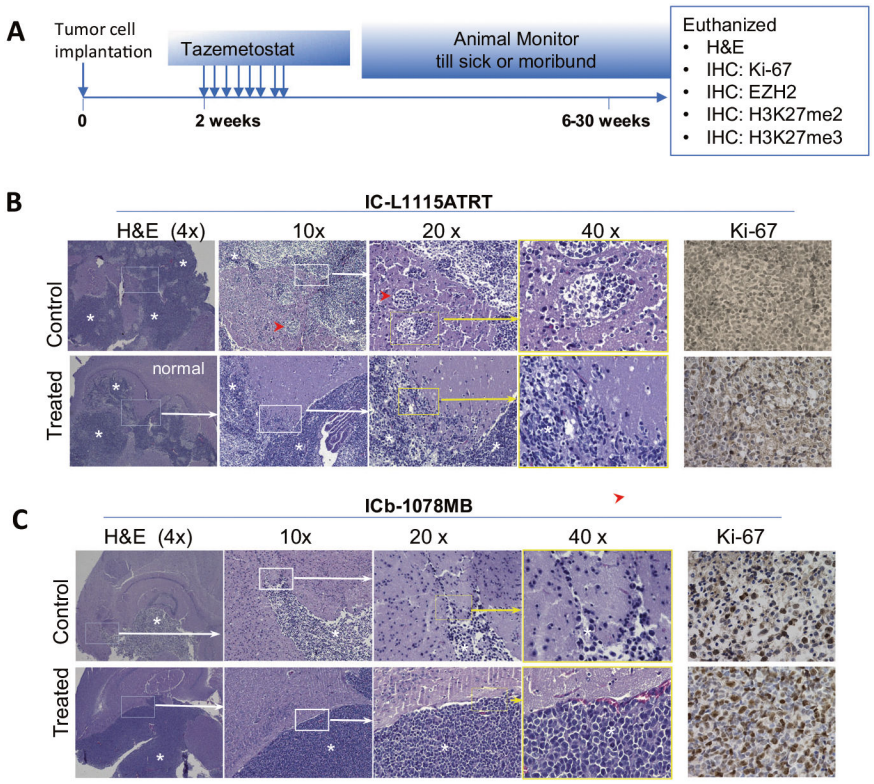

Fig. 4. Histological changes induced by tazemetostat.

A Schematic illustration of the timing of mouse brain collection after in vivo treatment. **B** H&E staining showing the in vivo growth of PDOX tumors (*) from low (4×) to high (40×). Compared with the untreated control, the remnant tumor of IC-L1115ATRT remained highly invasive although the number of satellite foci (*red arrowhead*) was slightly reduced (*upper panel*). The local invasion of IC-1078MB was not significantly affected (*lower panel*). Cell proliferation (Ki-67) in the remnant tumor was similar to the untreated controls.

Author Manuscript Author Manuscript Author Manuscript Author Manuscript

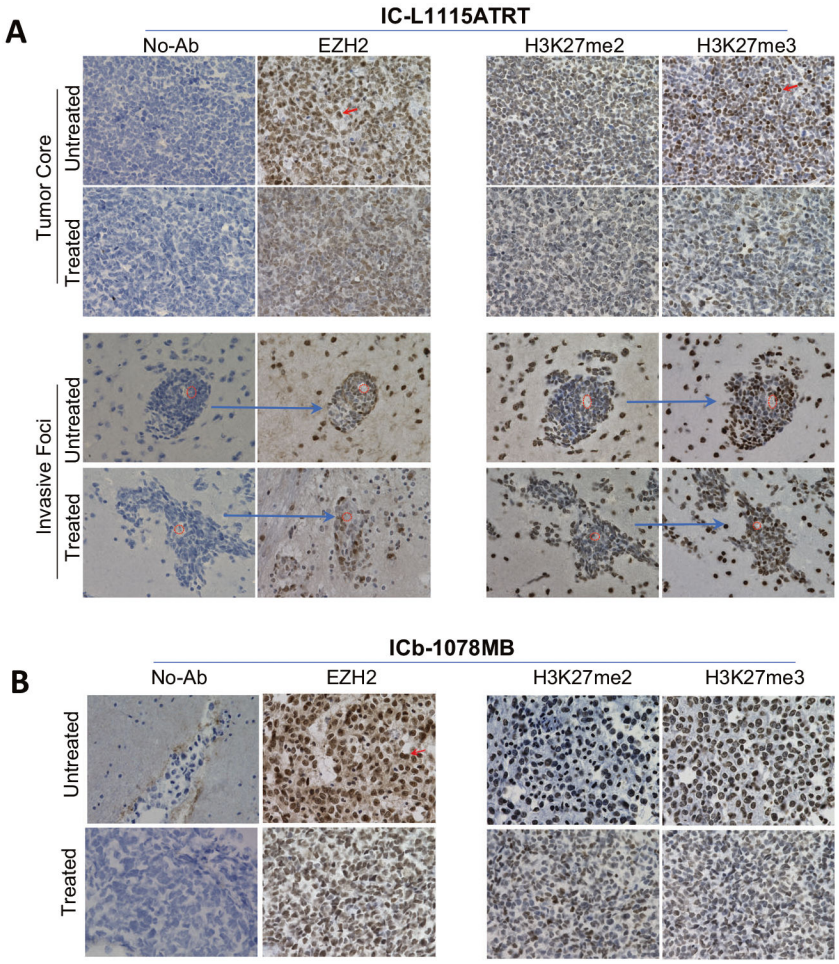

Fig. 5. Immunohistochemical staining of molecular targets of tazemetostat in vivo.

A In IC-L1117ATRT, strong positive staining (*arrow*) of EZH2, H3K27me2 and H3K27me3 were significantly reduced in the tumor core (*upper panel*) and in the remaining invasive foci (*lower panel*) accompanied by increased number of cells with low or no expression. Note that the same foci surround a micro-blood vessel (*red circle*) from the consecutive sections of the same tumor (*arrow*) were imaged and shown. **B** In IC-1078MB, the reduction of EZH2 strong positivity (*arrow*) was accompanied by the decrease of H3K27m3 expression in the remnant tumor.

Author Manuscript Author Manuscript Author Manuscript Author Manuscript

Table 1.

Clinical, histological, and molecular features of the PDOX models.

Model ID	Age/Gender	Diagnosis	Metastatic/ Recurrent	Molecular subtype			References
				Pt tumor	PDOX	Sequenced	
IC-2305GBM	9 y Female	GBM (small cell variant)	No/No	GBM-G34[a]	GBM-G34[a]	*TP53, H3F3A (G34R), ATRX* mutation	36,37
ICb-1078MB	11 y 9 mo Male	MB (anaplastic)	No/No	Group 4[a]	Group 4[a,b]	*MYC, N-MYC* amplification; P *DZRN4, SCNNIB,* and *KNTC1* mutation	35,36
ICb-1572MB	14 y 9 mo Male	MB (large cell)	Yes/No	Group 3[a]	Group 3[a,b]	*GARID1A* mutation	34,35
IC-L1115ATRT	3 m Male	ATRT (from autopsy)	Yes/Yes	SHH[a]	SHH[a]	*INI1* deletion	36

[a]With gene expression profiling.

[b]DNA methylation.

Lab Invest. Author manuscript; available in PMC 2023 May 30.